



Research Article

ISSN : 0975-7384
CODEN(USA) : JCPRC5

Green synthesis, characterisation and biological activities of silver nanoparticles by using *Wrightia tomentosa* leaves

Bodaiah B.¹, Usha Kiranmayi Mangamuri², Vijayalakshmi M.², V. S. Rama Krishna Ganduri^{1,3}, K. R. S. Sambasiva Rao¹ and Sudhakar Poda^{1*}

¹Department of Biotechnology, Acharya Nagarjuna University, Nagarjuna Nagar, Guntur - 522510, India

²Department of Botany and Microbiology, Acharya Nagarjuna University, Nagarjuna Nagar, Guntur-522510, India

³Department of Biotechnology, K. L. University, Green Fields, Vaddeswaram, Guntur-522502, India

ABSTRACT

The present study was aimed at green synthesis of silver nanoparticles (AgNPs) using aqueous leaf extract of an endangered plant *Wrightia tomentosa* at room temperature. Synthesis of WT-AgNPs was characterized by visual colour change of the reactants due to the reduction of AgNO₃ by the plant extracts which also act as capping agents. An intense band of Plasmon resonance was observed at ~454 nm in UV visible spectrum confirms the formation of WT-AgNPs. Study of the various functional groups of the biomolecules capping the AgNPs was confirmed by FTIR spectrum. XRD analysis reveals the degree of crystallinity and face centered cubic structure of the monophasic AgNPs. In addition, the shapes and nature of the AgNPs was also confirmed by SEM, while SEM-EDX confirmed the presence of elemental silver and TEM studies reveal the shape of the AgNPs. DLS revealed the mean size of the nanoparticles formed and measured 2.9 nm in monodispersed condition. Further the antimicrobial and Minimum Inhibitory Concentration (MIC) potency of the synthesized AgNPs was tested against pathogenic Gram positive, Gram negative bacterial and fungal strains that showed promising activity. Cytotoxicity of the WT-AgNPs was tested against MDA-MB-231, HeLa, MCF-7 and OAW-42 cancer cell lines.

Key words: Green synthesis, AgNPs, *Wrightia tomentosa*, Antimicrobial activity, MIC, Cytotoxicity.

INTRODUCTION

Indeed, nature is a natural nano workshop and has induced interest and attention of many researchers to probe into the mechanism behind the biosynthesis of silver nanoparticles (AgNPs) by plant and plant derived materials in addition to explore the reduction of silver and to understand the mechanism of AgNPs formation [1]. Ion sputtering, chemical reduction and sol gel etc are the prime methods employed for chemical synthesis of nano particles where high energy input and release of hazardous chemicals waste [2, 3]. Obviously it is very important to look around the alternative strategies that are cost effective and should be ecofriendly. Biological synthesis of AgNPs is the key procedure using natural products such as biopolymers, plant extracts and microorganisms as reductants and as capping agent's alternative to chemical synthesis [4].

Application of the environmental friendly green chemistry and chemical technologies is at great demand due to worldwide environmental concerns. Biological reductive synthesis of AgNPs with plant extracts has become significant due to their antimicrobial and cytotoxic properties [5, 6]. Hence their role can be projected as antimicrobial agents for future generation [7]. In addition, AgNPs find application in various fields such as bio-diagnosics, bio-sensing, microelectronics, imaging, designing new drugs [8], catalysis, photonics and electronics [9]. Methods adapted for green synthesis of AgNPs are simple, cost effective, one step, ecofriendly and the results are highly stable [10]. The rate of plant mediated synthesis of AgNPs is rapid than the microbes [11]. Hence plant

extracts have been identified as the viable source to other chemical methods [12]. Principles of green chemistry are safe and efficient and also minimize the chemical pollution.

Considering the potentiality of the plant as a source than the chemical methods for the synthesis of AgNPs, the work was aimed with green technology for the synthesis of AgNPs to that of chemical methods. In this process the leaf extract of *Wrightia tomentosa* (Roxb) *Roem and schult.* an endangered tiny deciduous tree of *Apocyanaceae* family is used for green synthesis of AgNPs. This plant grows in India and is commonly used as remedy against human ailments from antiquity such as stomach ache, tooth ache, arthritis and snake bite. The method is expeditious, ecofriendly and convenient method for the synthesis of silver nanoparticles using aqueous leaf extract of *W. tomentosa*.

EXPERIMENTAL SECTION

Materials:

All the materials procured were of analytical grade. The Silver nitrate (AgNO_3) with 99.5% purity was purchased from Merck. Fresh leaves of *W. tomentosa* have been collected from Tirumala hills, Tirupathi, Chittoor District, Andhra Pradesh, India. The plants were taxonomically identified and authenticated by Prof. M. Vijayalakshmi, Dean and Professor, Dept of Botany, Acharya Nagarjuna University, Guntur, Andhra Pradesh, India. Milli Q molecular grade water was used throughout the experiment.

Preparation of the plant material:

Fresh leaves of *W. tomentosa* were used for the preparation of the leaf extract. The collected leaves were initially washed through with tap water to remove dust and undesired particles, followed by second wash with molecular grade water and shade dried the leaves on a blotting paper for 10 days. The dried leaves were ground to fine powder with mortar and pestle. 2 grams of the leaf powder was mixed with 100ml of molecular grade water and heated up to 70 °C for 15 min. The reaction mixture was filtered through Whatman No 1 filter paper and the extract was stored at room temperature for further studies.

Green synthesis of silver nanoparticles:

10 ml of the prepared plant extract was mixed with varying concentrations (0.1mM, 0.5mM, 1mM and 2mM) of 190 ml of silver nitrate solution. The entire reaction was carried out in dark chamber to minimize the photo-activation of silver nitrate. The color change from colorless to brown confirms the formation of colloidal AgNPs and the formation of the AgNPs were confirmed by UV-Visible spectroscopy [11].

Characterization of the silver nanoparticles (WT-AgNPs):

Surface plasmon resonance analysis of WT-AgNPs:

Formation of the AgNPs was analysed by using Thermo Scientific Evolution 2001 (Isight software) spectrophotometer. Surface plasmon resonance (SPR) was observed in the visible region between 400 to 500nm. The λ_{max} values were recorded for every 15 min from the start of the experiment and after 24h to analyse the formation of the biogenic AgNPs. Formation of the AgNPs was plotted with wave length on the x-axis and absorbance on y-axis.

FTIR (Fourier transform infrared) analysis of WT-AgNPs:

The functional groups present in the phyto constituents in leaf extract of *Wrightia tomentosa* and their role in the biogenic synthesis of AgNPs were determined by the FTIR studies. The AgNPs were purified by centrifugation at 10,000 rpm for 30 min. The precipitate was washed thrice with molecular grade water and dried. The purified powder AgNPs was mixed with potassium bromide (KBr) to make a pellet and analysed by FTIR (Jasco FT/IR-6300 Fourier transform infrared spectrometer). FTIR analysis was executed to identify the phyto compound present in the leaf extract responsible for the reduction and stabilization of WT-AgNPs [13].

XRD studies of WT-AgNPs:

The biogenic WT-AgNPs colloidal powder was drop coated on to a glass substrate and the XRD measurements were carried out using Philips X'PERT Pro XRD instrument with the following working conditions; Voltage of 40kV, 30 mA, Cu $K\alpha$ Ni- filtered radiation in θ - 2θ configuration. XRD analysis is helpful for phase identification and characterization of nano-particle crystal structure [14]. X-rays penetrate the nanoparticles and the diffraction pattern obtained is compared with the standard to obtain structural information [15].

Energy dispersive X-ray spectroscopy (EDX):

Elemental composition of the sample is determined by EDX. EDX analysis confirms the presence of silver in the particles and also to detect the other elemental composition and their concentration in the synthesized WT-AgNPs.

10 μ l of the 100 fold diluted sample was placed on the carbon stub and air dried. The spectrum was obtained at an operation of 20kV. Completion of the mapping represents the two-dimensional spatial distribution of energy emissions of the chemical elements present in the sample. EDX analysis was completed using microprobe mounted scanning electron microscope [16].

Dynamic light scattering (DLS):

DLS also known as photon correlation spectroscopy or quasi elastic light scattering technique was applied for determining the size, distribution and particle's motion in the medium. Z-average hydrodynamic diameter of the sample was measured by using *Dynamic Light Scattering* (DLS) technique (HORIBA Z100 Nanopartica) at a scattering angle of 173°. Stokes-Einstein equation is applied for the calculation of the mean diameter of the particle. Polydispersity index (PDI) reveals the width of the particle size [17].

SEM and TEM analysis:

For Scanning Electron Microscopy analysis thin films of the WT-AgNPs suspension was prepared by dropping a small amount of the sample on the carbon coated copper grid. Excess sample was wiped out with blotting paper and the film is dried for 5 min using a mercury lamp and the images were taken in Zeiss Scanning electron microscope. SEM analysis confirms the presence and formation of silver nano particles. Transmission electron microscopy (TEM) analyse the details of the WT-AgNPs morphology. The aqueous leaf extract of the *Wrightia tomentosa* was subjected to sonication for 10 min, after which a drop of the WT-AgNPs colloidal solution was placed on the carbon coated copper grids and later exposed to infrared light for 30 min to dry up. These observations were carried out on Transmission electron microscope (PHILIPS model CM 200).

Kirby-Bauer Disc Diffusion assay for antimicrobial activities of WT-AgNPs:

Antimicrobial activity of the biogenic synthesized WT-AgNPs were tested against pathogenic bacterial and fungal strains such as Gram positive bacteria *Staphylococcus aureus* (MTCC 3160), *Salmonella paratyphi* (MTCC 3220), Gram negative bacteria *Escherichia coli* (MTCC 1683), *Xanthomonas campestris* (MTCC 2286) and pathogenic fungi *Aspergillus flavus* (MTCC 9367), *Candida albicans* (MTCC 7253), *Candida tropicalis* (MTCC 6192) and *Fusarium graminearum* (MTCC 2089) procured from Microbial type culture collection (MTCC), Chandigarh, India.

Antimicrobial activity was carried out by the cup-plate agar diffusion method [18]. The Mueller-Hinton agar (Bacteria) and Czapek Dox agar (Fungi) prepared and was inoculated with the pathogenic bacterial and fungal strains. 100 μ g/ml of the green synthesized WT-AgNPs were inoculated in to the wells of the petri plates and kept for incubation at 37 °C (Bacteria) and 28 °C (Fungi). The zone of inhibition (mm) was measured after 24 h. In each plate one well was loaded with plant extract and other with standard antibiotic. All the experiments were carried out in triplicate and the average value of the zone of diameter was recorded (Table 1).

MIC determination by micro-plate broth dilution method:

Sterile 200 μ l micro plates were used for the assay. Minimum Inhibitory Concentration of *E. coli*, *B. subtilis* and *S. aureus* was determined by micro titer broth dilution method using Mueller-Hinton Broth (Hi-media) [19]. Each micro titer well was loaded with broth (35 μ l) along with 1 μ l of bacterial inoculum as per (McFarland Nephelometer Standards), 50 μ l of molecular grade water and 10 μ l of WT-AgNPs (Test sample) of different concentrations (50 μ g, 45 μ g, 40 μ g, 35 μ g, 30 μ g, 25 μ g, 20 μ g) and kept for incubation at 37 °C for 24 h. 5 μ l of the p-INT (P-Iodonitrotetrazolium violet) as indicator developed by was added to each well and incubated for additional 2 h [20]. The MIC^{INT} was determined as the lowest concentration of test sample at which no red color (Signifying no growth) appeared. The A lane of the micro- plate was filled with 100 μ l molecular grade water and B, D and F lane of the micro-plate are loaded with bacteria plus 95 μ l of saline to act as controls. Lane C, E and G of the micro-plate were filled with bacterial culture, saline and AgNPs.

Cell proliferation (MTT) assay

Cytotoxicity of the green synthesized WT-AgNPs was measured based on the *in vitro* growth in the 96-microtitre plates by cell mediated reduction of tetrazolium salt to water insoluble formazan crystals as per the micro culture MTT assay [21]. Cell lines include human breast adenocarcinoma cell lines (MDA-MB-231), human cervical cancer cell lines (HeLa), human ovarian cyst adenocarcinoma cell lines (OAW-42) and human breast adenocarcinoma cell lines (MCF-7) (cell line reported to be resistant to cancer drugs) obtained from National Centre for Cell Science, Pune, India. Cell lines MDA-MB-231, HeLa and OAW-42 were cultured on Dulbecco's modified Eagle's medium supplemented with fetal bovine serum (10%; v/v), L-glutamine (2mM), penicillin (10 units/ml) and streptomycin (10 μ g/mL), while Breast cancer cell line MCF-7 was cultured on Roswell Park Memorial Institute medium 1640 supplemented with fetal bovine serum (10%; v/v), L-glutamine (2 mM), penicillin (10 units/mL) and streptomycin (10 μ g/mL) in a humidified atmosphere (95%) with 5% of CO₂ at 37°C.

Cells were seeded in 96-well micro titer plates at a density of 5×10^3 per well (100 μ l) containing 0.1 ml medium and subjected to overnight incubation. The cell lines were treated with different concentration of leaf extract (10, 25, 50, 75, 100, 150 mg/ml) and WT-AgNPs (20, 40, 60, 80, 100, 120, 140 μ g/ml) with triplicates of each concentration. After 24 h of incubation, the cell viability was assessed by adding 20 μ l of MTT (5mg/ml in PBS) per well and the plates were incubated at 37°C for 4 h. The formazan crystals formed in the cells were dissolved with 100 μ l of 0.1% acidified Isopropanol and the rate of color development was measured at 570 nm using a micro plate reader. The IC₅₀ value (50% inhibitory concentration) of the plant extract and AgNPs were calculated. Optical density values were converted to percentage of viability by using the following formula: Percentage of cell viability = $100 \times \text{OD value of experimental samples} / \text{OD value of experimental controls}$.

RESULTS AND DISCUSSION

Addition of *Wrightia tomentosa* leaf extract with aqueous solution of silver nitrate led to the observable change in the colour of the solution (Plant extract and AgNO₃ solution) from yellowish to reddish brown (Fig 1). A strong peak formed in the UV-Vis Spectrophotometer (Thermo Scientific) at 432 nm due to a strong Surface Plasmon resonance which indicates the formation of WT-AgNPs [1, 22]. Influence of different concentrations of the leaf extract was studied with varying volumes of the AgNO₃ (1mM) solution i.e. 2.5 ml, 2.0 ml, 1.5 ml, 1.0 and 0.5 ml of Plant extract was mixed with 17.5 ml, 18.0 ml, 18.5 ml, 19.0 ml, 19.5ml of AgNO₃ solution respectively. Formation of WT-AgNPs was observed when the reactive solution contained 19 ml of the AgNO₃ solution with 1ml of the plant extract and the change in the colour of the solution from faint light to yellowish brown and then to colloidal brown indicates formation of silver nanoparticles (Fig 2).

The synthesis was analysed and observed by UV-Vis spectrum of Surface Plasmon resonance band between 430-440 nm. These obtained results are in agreement with the results reported by Obaid *et al.* (2015) [23]. Minor spectral variation values signify the change in the particle size [24]. In addition, SPR band obtained due to influence of time on the formation WT-AgNPs, showed that the maximum peak was observed at 440nm after 8 h of incubation and gradually increased up to 48h. The PRS showed the spectrum values ranging between 425 to 440 nm which indicate the formation of AgNPs. The results obtained are in close proximity to the results reported, where the absorbance values are at 445 nm for the AgNPs synthesized from *Cochlospermum religiosum* extract [25] and *Pithophorae dogonia* extract [26]. SPR spectrum divulge that biogenic synthesis of WT-AgNPs was obtained from the leaf extract of *Wrightia tomentosa*.

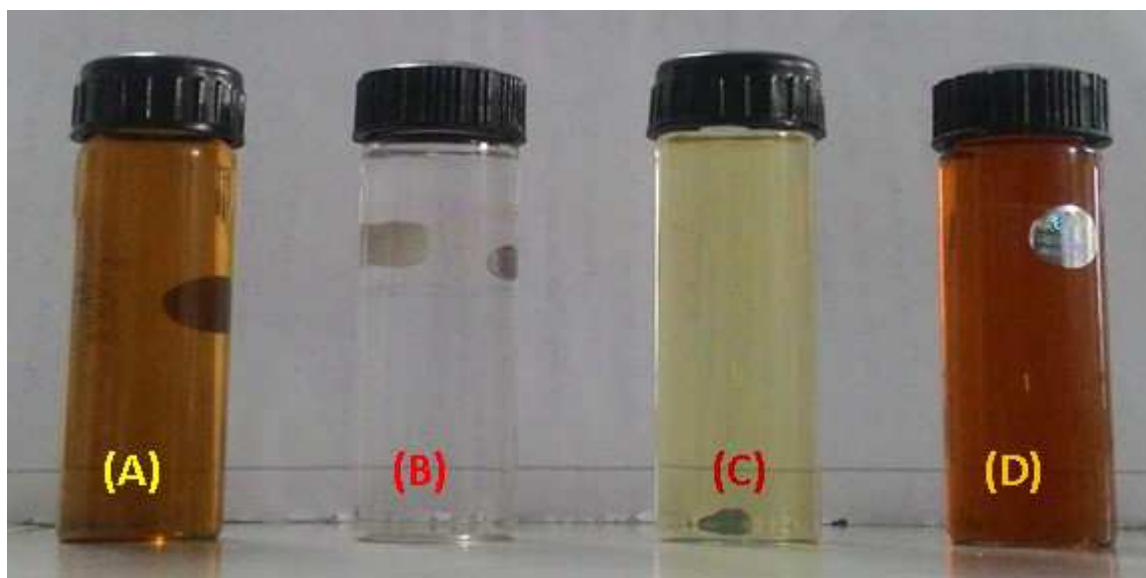


Fig. 1: Synthesis of *W. tomentosa* AgNPs where (A) plant extract (B) Silver nitrate (C) Plant extract plus silver nitrate at the start of incubation (D) AgNPs after 48hrs

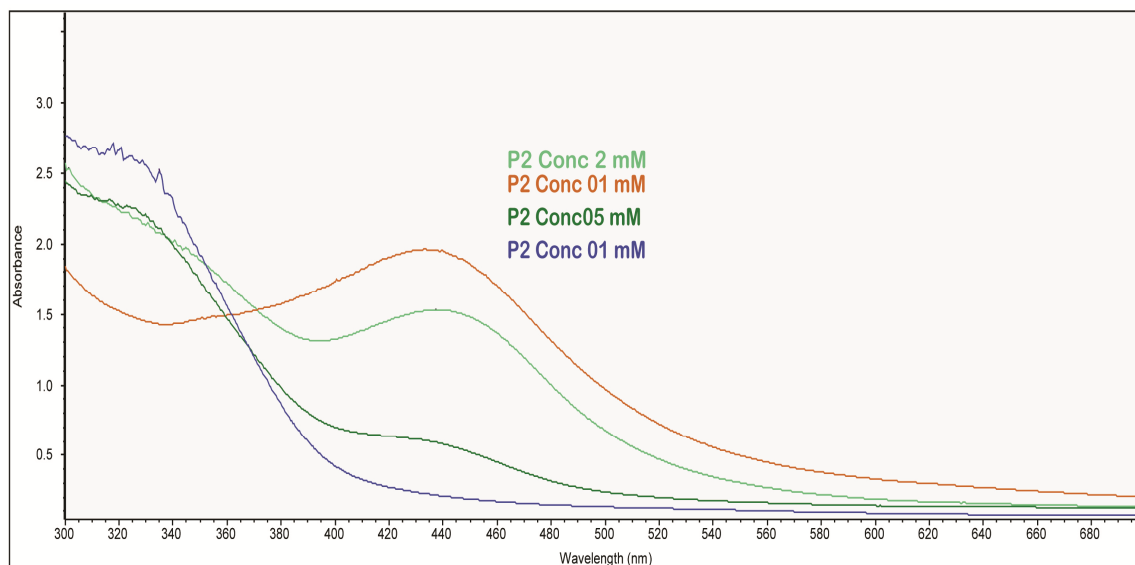


Fig. 2: Synthesis of *W. tomentosa* AgNPs using different molar concentrations of AgNO_3

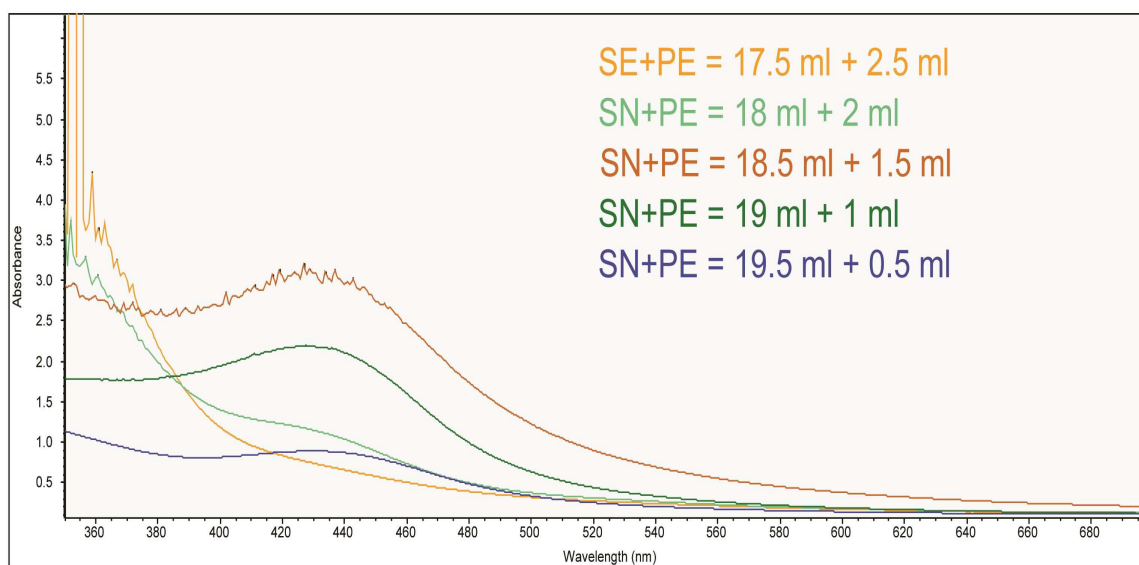


Fig. 3: Synthesis of *W. tomentosa* AgNPs using different concentrations of plant extract

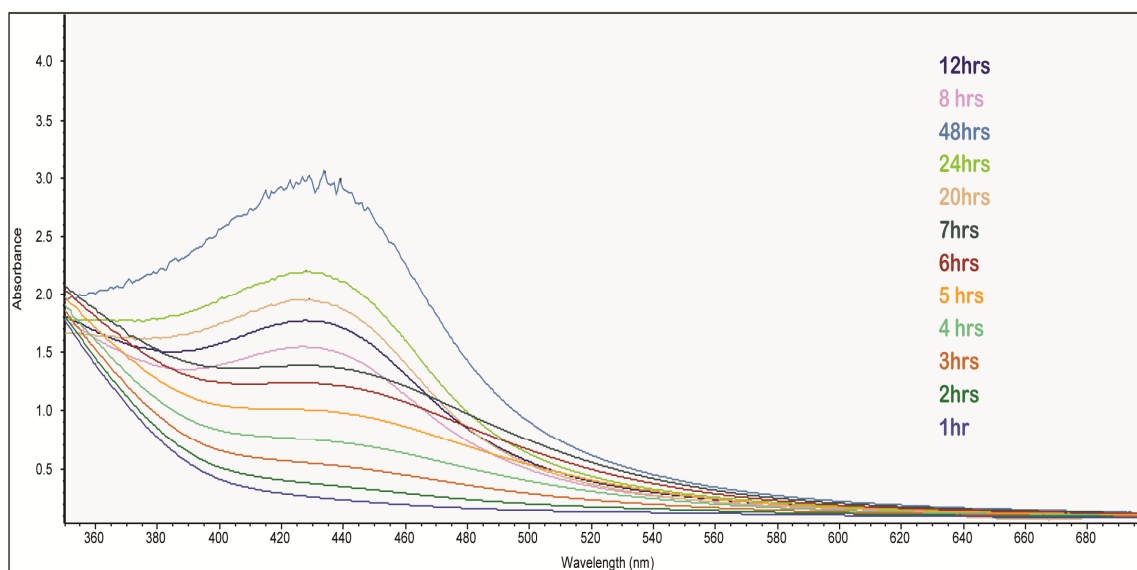


Fig. 4: Synthesis of *W. tomentosa* AgNPs at different time intervals

Fourier Transform Infrared Spectroscopic analysis:

FT-IR analysis characterizes and identifies the biomolecules that are specifically bound to synthesize WT-AgNPs. The leaf extract spectrum of *W. tomentosa* displayed a number of peaks that reflects the complex nature. The peak obtained at 3361.93 cm^{-1} is the result of O-H bond stretching of alcohols and phenols. The peaks at 2926.01 cm^{-1} and 715.59 cm^{-1} is assigned to the characteristic stretching vibrations of C-H stretch and C-H rock of alkanes. Peak 1624.06 are the stretching vibrations of N-H bend 1° primary amines. The peaks observed at 1074.35 and 1045.42 correspond to aliphatic amines while the peaks at 831.32 and 592.15 are characteristic of alkyl halides. Shift in these peaks and decreasing the band intensity revealed the fact that the tryptophan residues of the protein play an important role in reducing and stabilization of the AgNPs. These shifts in peak positions reveal the different phytochemicals present in the leaf extract of *W. tomentosa* and their presence in the stabilized AgNPs [27]. The results obtained are in corroborate with those found in literature [28]. Hence it can be concluded that bioorganic compounds of the *W. tomentosa* leaf extract formed a strong coating/capping on the biogenic AgNPs [11].

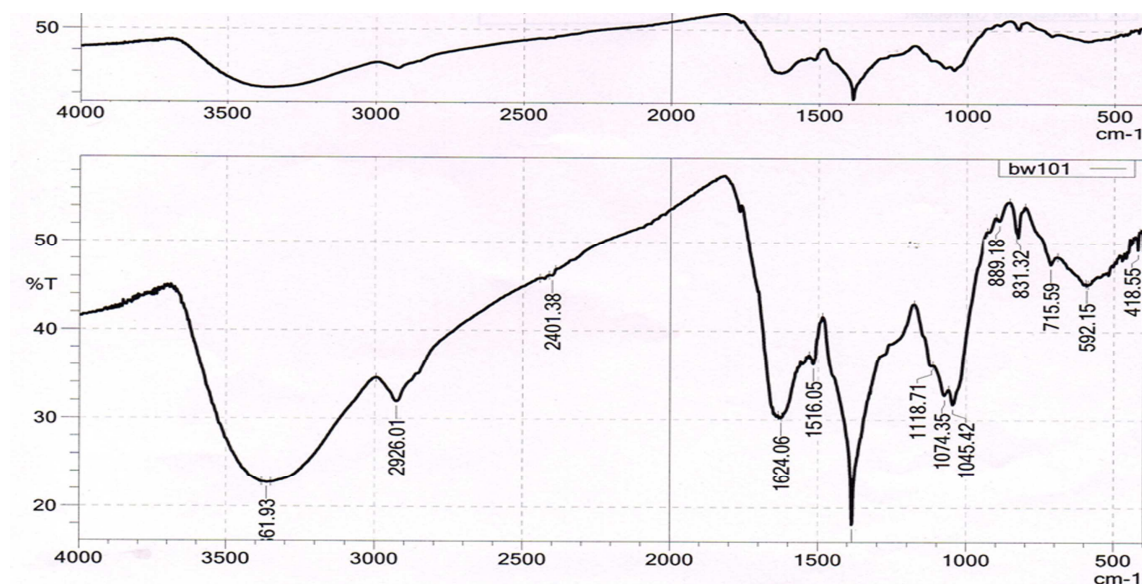


Fig. 5: FTIR spectrum of *W. tomentosa*

XRD Analysis:

The crystalline nature and the grain size of the synthesized WT-AgNPs were confirmed by X-ray powder diffraction (XRD). XRD spectrum of WT-AgNPs synthesized from the leaf extract of *W. tomentosa* showed Bragg peaks (angle 2θ) at 31.89 , 37.83 , 44.00 , 64.19 and 77.18 which corresponds to the indexed planes of 122 , 111 , 200 , 220 and 311

Miller indices which corresponds to the formation of face centered cubic (FCC) crystalline elemental silver. The unassigned peaks might be the crystalline bioorganic phases on the surface of the WT-AgNPs (29). Using Debye-Scherrer equation the average grain size of the biogenic synthesized WT-AgNPs was determined [$d = K\lambda / \beta \cos \theta$] where, 'd' is the mean diameter of the particle; 'K' is the shape factor (0.9); ' λ ' is the X-ray radiation source (0.154 nm); ' β ' is $(\pi / 180) * \text{FWHM}$ and ' θ ' is the Bragg angle which was 17.7 nm [6].

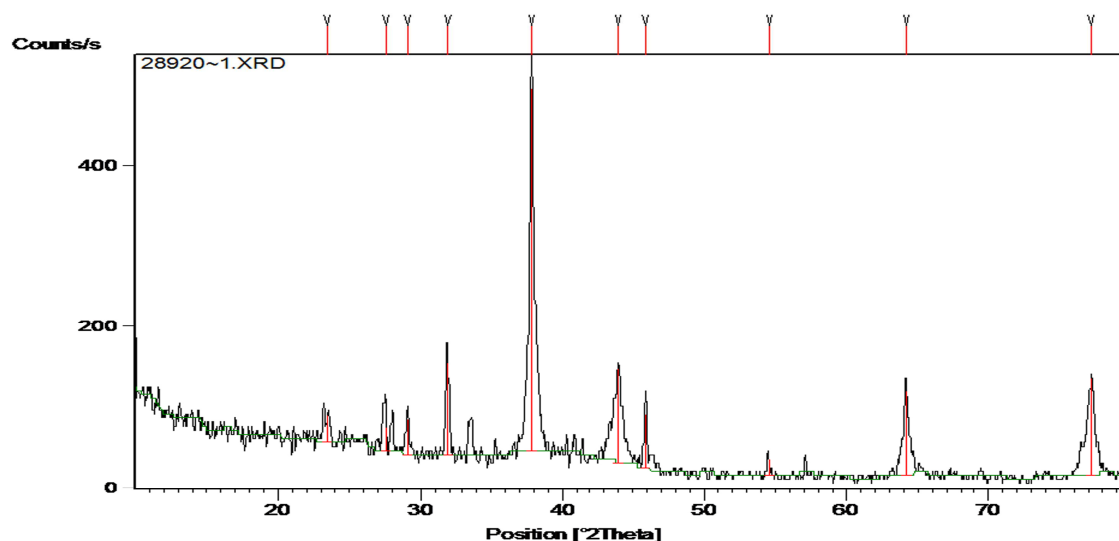


Fig. 6: XRD spectrum of *W. tomentosa* AgNPs

SEM/EDX study:

The EDX spectrum of green synthesized WT-AgNPs is represented in (Fig. 7). The spectrum shows strong silver signal from the WT-AgNPs with quantitative percentage of 25.12%. The absorption peak is approximately 3 eV (410 nm) which is in accordance to the peak obtained due to plasmon resonance typical for metallic silver nanocrystals [30]. The weaker signals correspond to quantitative % of Carbon (C), Oxygen (O), Chlorine (Cl), Sodium (Na) and Potassium (K) was found to be 7.96%, 52.85%, 5.12%, 1.91% and 7.04% respectively [31]. Carbon signal comes from the adsorbed components of the leaf extract and signals of O, Cl, P may be due to adsorption of plant elements over WT-AgNPs. The signal of O may be partly from atmosphere or from -OH of NaOH (pH adjustment) and Na signal from the NaOH (pH adjustment) [32].

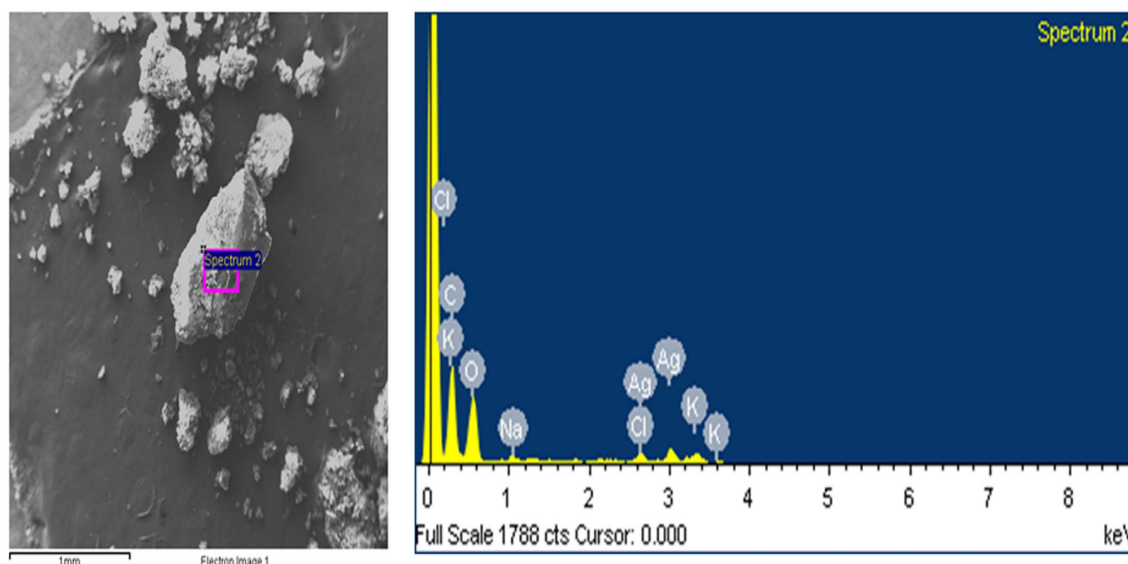


Fig 7: EDX spectrum of *W. tomentosa* AgNPs

Dynamic light scattering (DLS):

To probe the hydrodynamic size of the WT-AgNPs in colloidal aqueous environment, dynamic light scattering (DLS) studies were conducted. The particles exhibit brownian motion when dispersed in the medium which is measured by the fluctuations in the intensity of scattered light in the system from which translational diffusion coefficient is calculated by applying Stokes-Einstein equation which determines the hydrodynamic size [33]. The analysis was executed at 25 °C in a standard monodispersed medium maintained at a viscosity of 0.892 m Pa·s. The

graph shows that almost equal size distribution below 5 nm for silver particle synthesized using 1mM of silver nitrate solution.

The mean size of the particles calculated for silver nano particles was 2.9 nm [34]. A PDI value more than 0.5 refers to the aggregation of the particles [35]. The WT-AgNPs synthesized showed a PDI value of 0.363 which clearly indicate that the particles are in monodispersed phase with very low chances of aggregation. Polydispersity index represents the ratio between different size to total number of particles [36].

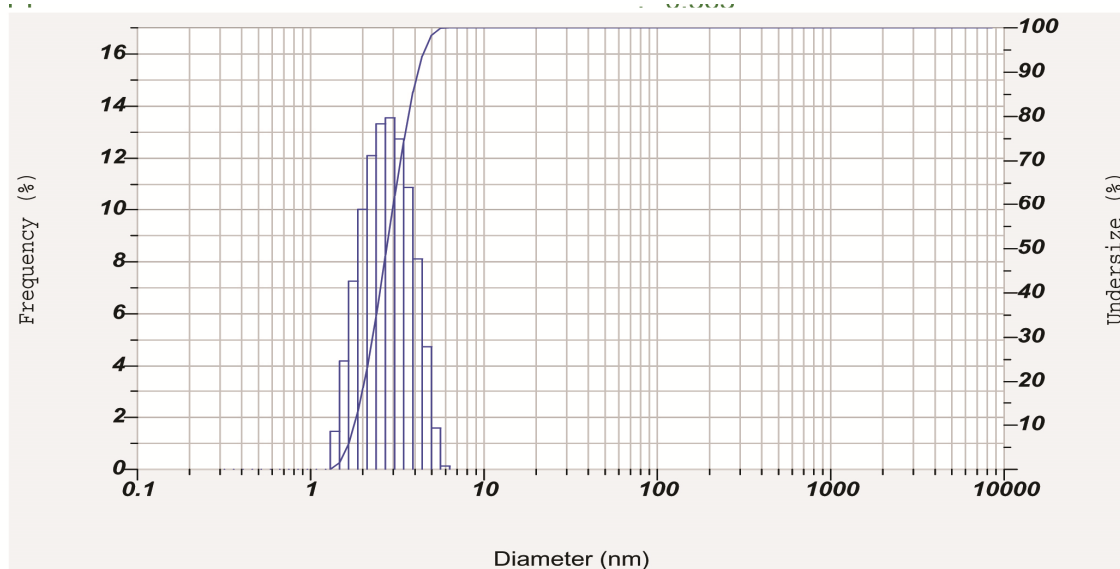


Fig 8: dynamic light scattering *W. tomentosa* AgNPs

Scanning electron microscopy:

Biogenic synthesized WT-AgNPs are subjected to characterization to study the morphology and size by SEM. The SEM analysis reveals that the WT-AgNPs have spherical shape. In addition, there were traces of WT-AgNPs cluster which arises due to aggregation of nanoparticles which might be induced due to evaporation of the solvent during the sample preparation [37]. In addition, the WT-AgNPs aggregation may be due to small gauges, high surface activity and large specific area of the nano particles [38]. The mean diameter of the WT-AgNPs was found to be 10-12 nm.

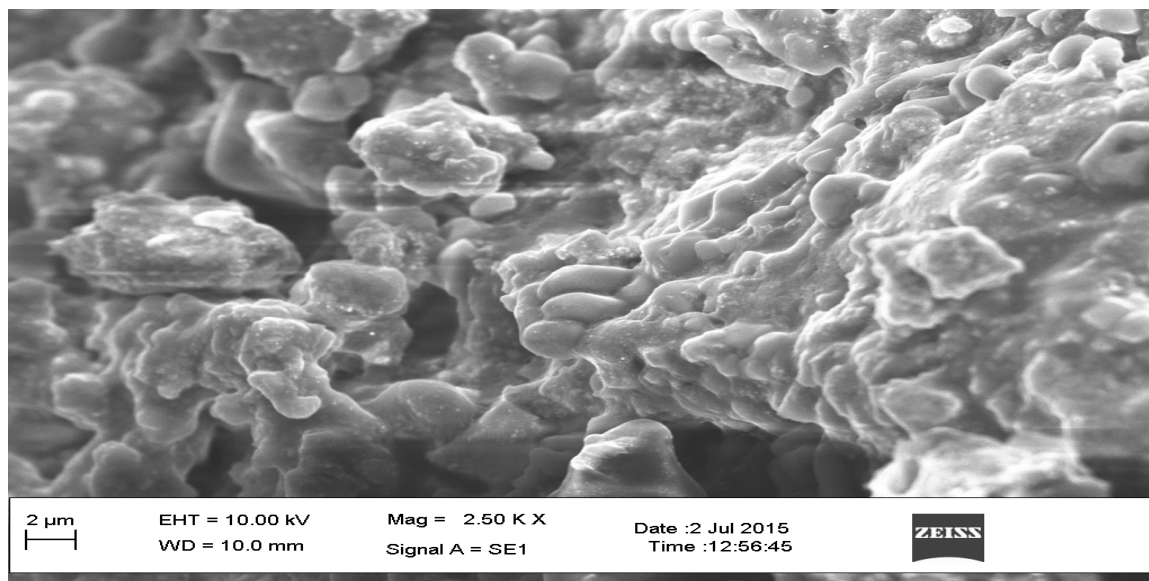


Fig. 9: SEM image of *W. tomentosa* AgNPs

Transmission Electron Microscopy (TEM):

Size and shape of the green synthesized WT-AgNPs was studied using TEM technique. Fig. 11 shows lattice fringes clearly. These particles appear to be nearly spherical shaped particles with smooth edges with a diameter nearly 10-12 nm. It was also found that the nanospheres are bounded with thin layer of biomolecule blanket on their surface which acts as stabilizing agent. Therefore, the particles were polydispersed with out direct contact and reliable for longer periods of time [39].



Fig. 10: TEM image of *W. tomentosa* AgNPs

Antimicrobial activity:

AgNPs have been reported to possess the antimicrobial properties and have wide applications in medicine, health industry, textile coatings, dye reduction, wound dressing food storage, antiseptic creams and environmental applications [40]. Elemental silver and its compounds have been used as antimicrobial agents since ancient times [41]. Antimicrobial potential of the biogenic WT-AgNPs were examined against Gram positive *Staphylococcus aureus* (MTCC 3160), *Salmonella paratyphi* (MTCC 3220), Gram negative bacteria *Escherichia coli* (MTCC 1683), *Xanthomonas campestris* (MTCC 2286) and pathogenic fungi *Aspergillus flavus* (MTCC 9367), *Candida albicans* (MTCC 7253), *Candida tropicalis* (MTCC 6192) and *Fusarium graminearum* (MTCC 2089) which were procured from Microbial type culture collection (MTCC), Chandigarh, India, has shown the zone of inhibition. The maximum zone of inhibition was observed against *X. campestris* (23 mm) and minimum was recorded against *E. coli* (17 mm).

Based on the zone of inhibition, the green synthesized WT-AgNPs proved to exhibit potent antimicrobial activity. Antimicrobial property of silver is already known and is used as positive control, in addition Streptomycin is used as standard reference and the plant extract did not document any antimicrobial activity (Fig. 11). AgNPs antimicrobial property is well documented but mode of action is debatable. Architectural difference between the cell wall peptidoglycan of Gram positive bacteria which is thin and facilitate easy entry of the AgNPs in to these cells while the peptidoglycan layer of the Gram negative bacteria is rigid where entry of AgNPs is difficult [42].

Ivan and Branka, (2004) has proposed that the AgNPs have the ability to attach to the cell membrane and cause the structural changes leading to the formation of the pits that facilitate their entry [43]. Initial no of bacteria and concentration of nanoparticles also influence the zone of inhibition. The effect of WT-AgNPs on ribosomes or suppression or expression of different enzymes and proteins that are actively involved in cell metabolism [6]. Antimicrobial activity results of the WT-AgNPs are shown in the Table 1. Efficient activity was recorded due to the large surface area of WT-AgNPs for better contact with cell wall of microbes [44]. The AgNPs also release silver ions generating an amplified biocidal effect on size and dose dependent [45].

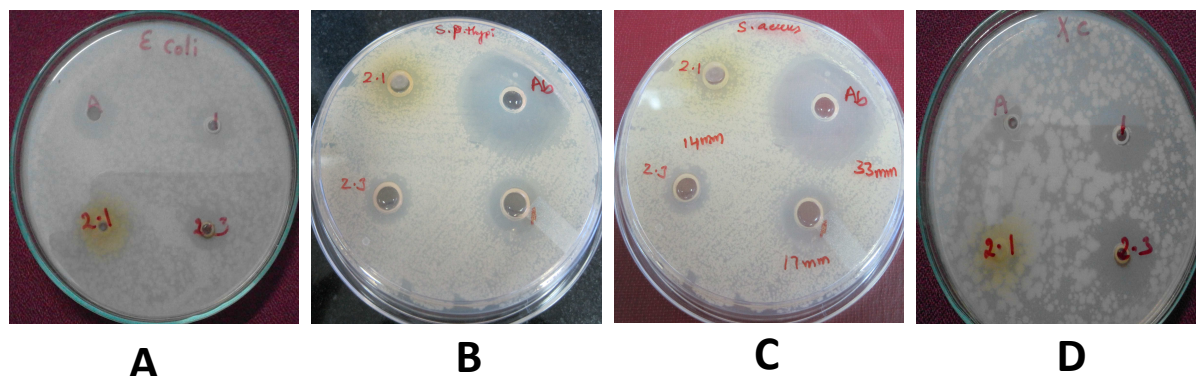


Fig. 11: Antibacterial activity of *W. tomentosa* AgNPs on (A) *E. coli* (B) *S. paratyphi* (C) *S. aureus* (D) *X. campestris* where the numbering 1, 2.1, 2.3, Ab or A shown on the plates codes for Silver nitrate, Plant extract, AgNPs and standard antibiotic Streptomycin respectively.

Table 1: Antibacterial activity (Zone of inhibition in mm)

Name of the bacteria	leaf extract	AgNO ₃	AgNPs 18 µg/100 µl	Streptomycin 20 µg/100 µl
<i>E. coli</i>	Nil	Nil	17	17
<i>S. paratyphi</i>	Nil	12	19	31
<i>S. aureus</i>	Nil	175	19	33
<i>X. campestris</i>	Nil	18	23	05

Antifungal activity of WT-AgNPs:

A significant antifungal activity of WT-AgNPs was recorded against *Candida albicans* which shows a maximum mean diameter of zone of inhibition of 25 mm and minimum of 15 against *Fusarium graminearum*. The standard drug Griseofulvin showed a maximum zone of 28 mm against *Candida albicans* and a minimum of 19 mm against *Fusarium graminearum*. Antifungal effect of the AgNPs synthesized is due to the inactivation of the sulfhydryl groups in the cell wall of fungi that leads to formation of insoluble compounds and also inactivates the vital cell membrane bound enzymes and lipids that result in cell lysis [46].

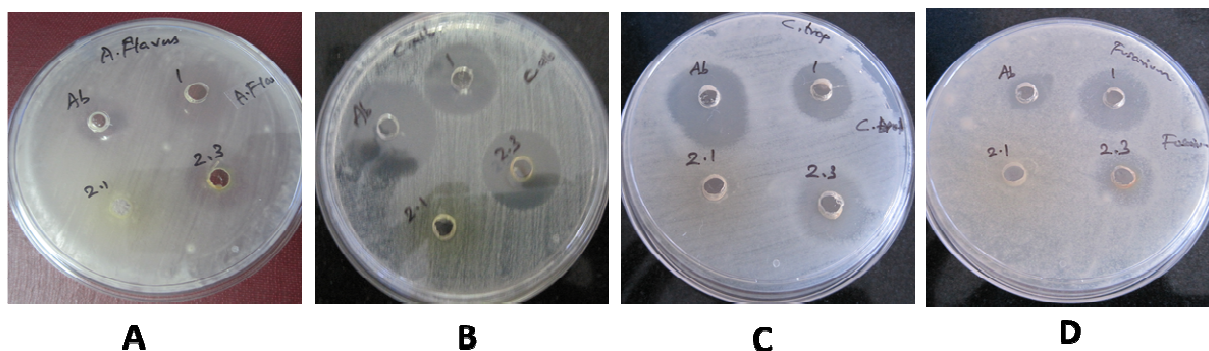


Fig. 12: Antifungal activity of *W. tomentosa* AgNPs on (A) *A. flavus* (B) *C. albicans* (C) *C. tropicalis* (D) *F. graminearum* where the numbering 1, 2.1, 2.3, Ab shown on the plates codes for Silver nitrate, Plant extract, AgNPs and standard antifungal agent respectively.

Table 2: Antifungal activity of *W. tomentosa* AgNPs (Zone of inhibition in mm)

Name of the fungi	leaf extract	AgNO ₃	AgNP _s	Griseofulvin
<i>Aspergillus flavus</i>	Nil	14	17	14
<i>Candida albicans</i>	Nil	19	25	28
<i>Candida tropicalis</i>	Nil	14	18	27
<i>Fusarium graminearum</i>	Nil	15	15	19

Minimum Inhibitory Concentration of WT-AgNPs:

MIC of the green synthesized WT-AgNPs are shown in Fig. The micro-plate inoculated with *E. coli*, *B. Subtilis* and *S. aureus* displayed the MIC even with the lowest concentration taken 25µg/µl. A concentration dependent inhibition of the test organisms growth was observed as the WT-AgNPs concentration were increased. This is the first report to determining the MIC of WT-AgNPs using P-Iodonitrotetrazolium reagent.

MTT assay:

Cytotoxic activity of the WT-AgNPs was measured against MDA-MB-231, HeLa, MCF-7 and OAW-42 cell lines with concentration ranging from 20 μg to 140 μg (20, 40, 60, 80 and 100 μg) and the cell viability was measured using MTT assay (Fig 13). The result was expressed in IC_{50} . The IC_{50} value of the WT-AgNPs against MDA-MB-231 (60 $\mu\text{g}/\text{ml}$, 47.2% of the cells are live) HeLa (60 $\mu\text{g}/\text{ml}$ where 38.4% of the cells are live), MCF-7(100 $\mu\text{g}/\text{ml}$ where 48.3% of the cells are live) and OAW-42 (100 $\mu\text{g}/\text{ml}$ where 45.6% of the cells are live). The percentage of the viable cells decreased with increase in concentration of WT-AgNPs in dose dependent manner [27]. Cytotoxic effects of silver are the result of active physicochemical interaction of silver atoms with the intracellular proteins as well the nitrogen bases and phosphate groups of the DNA [47].

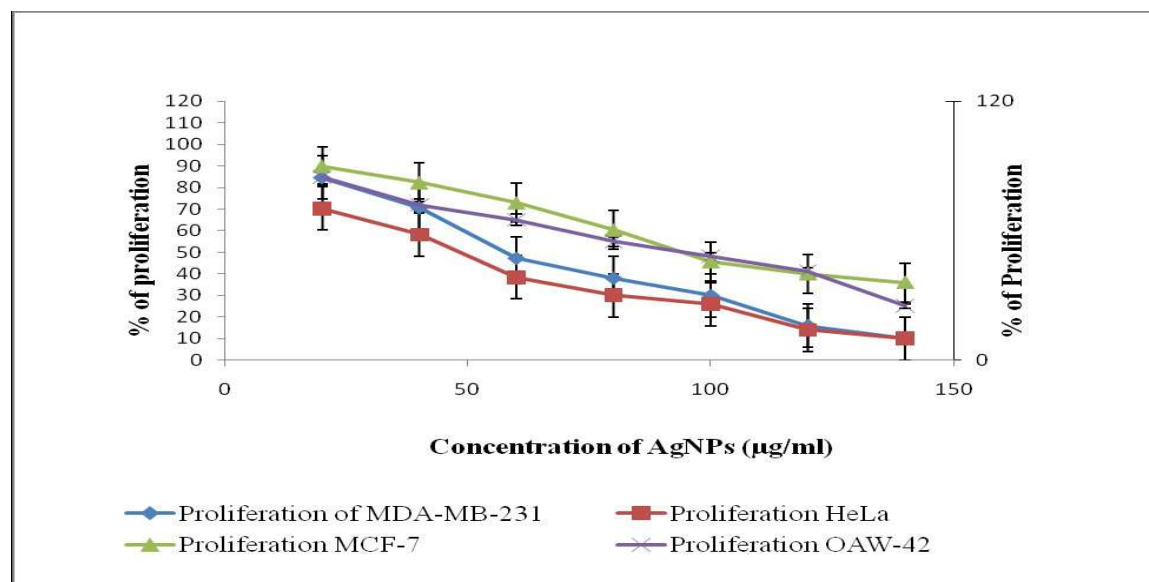


Fig. 13: MTT Assay of the WT-AgNPs against MDA-MB-231, HeLa, MCF-7 and OAW-42

CONCLUSION

The present study describes the reductive green biosynthesis of silver particles at nano-size using the leaf extract of *Wrightia tomentosa*, a relatively new and different approach. This green approach utilizes the natural, renewable and low cost biological reducing agent to produce metal nano particles in aqueous solution at room temperature eliminating the use of hazardous and toxic solvents. Green synthesized nanoparticles were characterized by UV-Vis spectrophotometer, FTIR, XRD, DLS, SEM-EDX, SEM, TEM.

The average mean size of the WT-AgNPs was found to be 2.9 nm in size in monodispersed condition. In addition the biogenic WT-AgNPs were further recorded antibacterial and antifungal activities against Gram positive, Gram negative bacteria and fungal pathogens. The MIC of the WT-AgNPs was recorded using P-Iodonitrotetrazolium as indicator. Cytotoxic activity of the WT-AgNPs was recorded against MDA-MB-231, HeLa, MCF-7 and OAW-42 and their IC_{50} values were expressed. The growing resistance of the pathogen to conventional antibiotics and the incidence of cancer demand the need for the novel molecules to combat. Nanoparticles express entirely a different mechanisms of antibacterial activity than to traditional antibiotics is compelling alternative tool in medicine.

Acknowledgements

The authors are thankful to the University Grants Commission (UGC)-RGNF, Govt. of India for providing financial support and the Department of Biotechnology, Acharya Nagarjuna University, Guntur for providing research facilities.

REFERENCES

- [1] Hanumanta R; Lakshmidhevi N; Pammi SVN; Pratap K; Ganapaty S; Lakshmi P; *Materials Science and Engineering: C*, **2016**, 62, 553–557.
- [2] Bindhu MR; Umadevi M, *Spectrochimica Acta Part A: Molecular and Biomolecular Spectroscopy*, **2015**, 135, 373-378.
- [3] Shakeel A; Mudasir A; Babu Lal S; Saiqa I, *Journal of Advanced Research*, **2016**, 7, 17–28.
- [4] Oxana VK; Rasika Dias HV; Kharisov BI; Betsabee OP; Victor MJP, *Trends in Biotechnology*, **2013**, 31, No. 4.

- [5] Ajitha B; Ashok Kumar Reddy Y; Shameer S; Rajesh KM; Suneetha Y; Sreedhara Reddy P, *Journal of Photochemistry and Photobiology B: Biology*, **2015**, 149: 84–92.
- [6] Debasis N; Sarbani A; Pradipta RR; Manisha K; Bismita N, *Materials Science and Engineering C*, **2016**, 58, 44–52.
- [7] Mohammad, J.H., Katharina, M.F., Ali Akbar, A., Dorleta Jimenez de, A., Idoia Ruiz de, L., Teofilo, R., Vahid, S., Wolfgang, J.P., Morteza, M., *Trends in Biotechnology*, **2012**, Vol. 30: 299-511.
- [8] Sneha, M., Oluwatobi, S.O., Soney, C.G., Jayachandran, V.P., Francis, B. L., Sandile, P.S., Nandakumar, K., Sabu, Th. *Carbohydrate Polymers*, **2014**, 106: 469–474.
- [9] Stalin, D.T., Ganesh Kumar, V., Karthick, V., Jini Angel, K., Govindaraju, K. *Spectrochimica Acta Part A: Molecular and Biomolecular Spectroscopy*, **2014**, 120: 416–420.
- [10] Jitendra, M., Amla, B., Abhijeet, S., Madan Mohan, S. *Advances in Natural Sciences: Nanoscience and Nanotechnology*, **2014**, 5: 043002.
- [11] Shakeel, A., Saifullah, M.A., Babu Lal, S., Saiqa, I, *Journal of Radiation Research and Applied Sciences*, **2016**, 9: 1 -7.
- [12] Prashant, M., Nisha, K.R., Sudesh, K.Y. , *J Nanopart Res*, **2008**, 10:507–517.
- [13] Sathishkumar, G., Pradeep, K.J., Vignesh, V., Rajkuberan, C., Jeyaraj, M., Selvakumar, M., Rakhi, J., Sivaramakrishnan, S., *Journal of Molecular Liquids*, **2016**, 215: 229–236.
- [14] Sun, S., Murray, C., Weller, D., Folks, L., Moser, A. *Science*, **2000**, 287:1989–92.
- [15] Amit Kumar, M., Chisti, Y., Chand Banerjee, U. *Biotechnology Advances*, **2013**, 31: 346–356.
- [16] Majumdar, R., Bag, B.G., Maity, N. *Int. Nano Lett*, **2013**, 3: 53.
- [17] Marcela, E.B.P., Nicoleta, B., Camelia, U., Marioara, C., Cristian, P., Ileana, R. *Optical Materials*, **2016**, 56: 94–99.
- [18] Jae, Y. S., Beom, S.K., *Korean J. Chem. Eng*, **2008**, 25 (4): 808–811.
- [19] Lakshmana Swamy, P., Rao, T.S., Arun Kumar, L.C., Srinivasa Prasad, Ch., Rao, G.S. *International Journal of Pharmacy and Pharmaceutical Sciences*, **2011**, Vol 3, Issue 4, 3: 436-440.
- [20] Eloff, JN. *Planta Med*, **1998**, 64 (8): 711-713.
- [21] Mosmann, T. *J. Immunol. Met*, **1983**, 65-55.
- [22] Ravichandran, V., Tiah Zi, Xi., Subashini, G., Wei Xiang, T.F., Chou Yang, E.F., Jeyakumar, N., Dhanaraj, S.A. *Journal of Saudi Chemical Society*, **2011**, 15: 113–120.
- [23] Obaid, A.Y., Al-Thabaiti, S.A., Al-Harbi, L.M., Khan, Z. *Global Advanced Research Journal of Microbiology*, **2015**, 3: 119-126.
- [24] Tripathy, A., Ashok, M.R., Chandrasekaran, N., Prathna, T.C., Mukherjee, A. *J Nanopart Res*, **2010**, 12:237–246.
- [25] Sasikala, A., Linga Rao, M., Savithamma, N., Prasad, T. N. V. K. V. *Appl Nanosci*, **2015**, 5:827–835.
- [26] Sankar Narayan, S., Dipak, P., Nilu, H., Dipta, S., Samir Kumar, P, *Appl Nanosci.*, **2015**, 5:703–709.
- [27] Sutanuka, P., Rahaman Mollick, M.M., Dipanwita, M., Sharmila, Ch., Sandeep Kumar, D., Sourav, Ch., Somenath, R., Dipankar, Ch., Mukut, Ch. *Journal of Saudi Chemical Society* , **2015**, doi:10.1016/j.jscs.2015.11.004.
- [28] Mahdi, S., Taghdiri, M., Makari, V., Rahimi, N.M. *Spectrochimica Acta Part A: Molecular and Biomolecular Spectroscopy*, **2015**, 136: 1249–1254.
- [29] Garima, S., Riju, B., Kunal, K., Ashish Ranjan, S., Pal Singh, R. *Journal of Nanoparticle Research*, **2011**, 13: 2981-2988.
- [30] Nikolić, M.V., Mijajlović, M.Ž., Jevtić, V.V., Ratković, Z.R., Radojević, I.D., Čomić, Lj.R., Novaković, S.B., Bogdanović, G.A., Trifunović, S.R., Radić, G.P. *Polyhedron*, **2014**, 79: 80-87.
- [31] Clearfield, A., Reibenspies, J., Bhuvanesh, N. *Principles and Applications of Powder Diffraction*, Wiley, **2008**.
- [32] Balaram, Das., Sandeep Kumar, D., Debasish, M., Totan, G., Sourav, Ch., Satyajit, Tr., Sabyasachi, D., Sankar Kumar, D., Debasis, D., Somenath, Roy. *Arabian Journal of Chemistry*, **2015**.
- [33] Barbara, J.F. *Appl. Opt.*, **2001**, 40: 4087-4091.
- [34] Vivek, D., Soumya, L., Bharadwaj, S., Shilpa, C., Deepika, B., Sreedhar, B., *Materials Science and Engineering C*, **2016**, 58: 36–43.
- [35] Nayak, B., Ray, A.R., Panda, A.K., Ray, P. *J. Biomater. Appl*, **2011**, 25: 469–496.
- [36] Kalainila, P., Subha, V., Ernest Ravindran, R.S., Sahadevan, R. *Asian J. Pharm. Clin. Res*, **2014**, 7: 39–43.
- [37] Ramesh, P.S., Kokila, T., Geetha, D. *Spectrochimica Acta Part A: Molecular and Biomolecular Spectroscopy*, **2015**, 142: 339–343
- [38] Soheila, M., Shahram, P., Abbas, A. *Journal of Environmental Chemical Engineering*, **2016**, 4: 2023–2032.
- [39] Vignesh, K.F., Anbarasi, S., Karthikeyeni, G., Sathiyarayanan, G., Subramaniana, P., Thirumurugan, R. *Colloids Surf. A: Physicochem. Eng. Aspects*, **2013**, 439: 184–192.
- [40] Xiugong G, Jeffrey JY, Vanessa, DT, Thomas B., Nicholas, O., Zachary, K., Robert, L.S. *Toxicology Reports*, **2015**, 2: 341–350
- [41] Lamabam SD; Joshi SR, *Journal of Microscopy and Ultrastructure*, **2015**, 3, 29–37.

- [42] Madigan M; Martinko J, *Brock Biology of Microorganisms*, Prentice Hall, Englewood Cliffs, NJ (11th ed), **2005**.
- [43] Ivan S; Branka Salopek S, *Journal of Colloid and Interface Science*, 2004, 275, 177–182.
- [44] Haytham MM, *Journal of Radiation Research and Applied Sciences*, **2015**, 8, 265-275.
- [45] Marambio JC; Hoek EMV, *Journal of Nanoparticle Research*, **2010**, 12, 1531-1551.
- [46] Jaidev LR; Narasimha G, *Colloids and Surfaces B: Biointerfaces*, **2010**, 81, 430–433.
- [47] Blagoi YP; Sorokin VA, *Stud. Biophysica*, **1991**, 128, 81.